

# Effect of alumina addition on the microstructure properties of plasma-sprayed zirconia-alumina coatings

SERKAN ISLAK\*

*Kastamonu University, Faculty of Engineering and Architecture, Department of Materials Science and Nanotechnology Engineering, 37000, Kastamonu, Turkey*

ZrO<sub>2</sub>/Al<sub>2</sub>O<sub>3</sub> coatings with different amounts of Al<sub>2</sub>O<sub>3</sub> were fabricated on the AISI 304 stainless steel surface using plasma spray process. Phase composition and microstructure of the coatings were characterised using X-ray diffraction and scanning electron microscopy. Lamellae and porous microstructure were obtained in the coatings. In addition, a small amount of unmelted particles, partially melted, and fully melted regions in microstructure of coatings were observed. With the increasing addition of Al<sub>2</sub>O<sub>3</sub>, a decrease in the pores was determined. The results indicated that the as-prepared ZrO<sub>2</sub>/Al<sub>2</sub>O<sub>3</sub> based coatings were mainly composed of ZrO<sub>2</sub>, Al<sub>0.52</sub>Zr<sub>0.48</sub>O<sub>1.74</sub>, ZrTiO<sub>4</sub>, Al<sub>0.18</sub>Zr<sub>0.82</sub>O<sub>1.91</sub>, Al<sub>2</sub>O<sub>3</sub>, Al<sub>2</sub>Zr<sub>3</sub>, Al<sub>3</sub>Ti and Ti<sub>2</sub>O<sub>3</sub> phases. The microhardness of the coating was as high as 1136 HV<sub>0.2</sub>, which was 4-5 times of the substrate.

(Received October 6, 2012; accepted July 11, 2013)

*Keywords:* Plasma spray, ZrO<sub>2</sub>, Al<sub>2</sub>O<sub>3</sub>, Microstructure

## 1. Introduction

Plasma spray is applied efficiently and economically on several machine parts in order to reduce the degradations on the surface [1-4]. Completely or partially melting of powders varies depending on their thermal properties in this method. The system's controllability in extremely high heating and cooling rates enables producing metallic, non-metallic and ceramic-based coatings through this method [5]. In plasma spray method, oxide based powders are used more frequently compared to metallic powders due to their chemical stability in high temperature, excellent wear resistance and corrosion resistance [6]. Bonding of coating layer to the substrate does not have metallic character in oxide-based coatings. The fact that oxide coatings have ionic bond character prevents the formation of compliant lattice planes in the intermediate layer. Stress concentration occurs in the coating as a result of this. In order to prevent this negative effect, it is useful to use a thin intermediate layer. By using intermediate layers, the change in the thermal expansion coefficient gradient between the oxide based coatings obtained and the substrate is minimised [7-11].

Al<sub>2</sub>O<sub>3</sub>-TiO<sub>2</sub> coatings are widely fabricated by plasma spray system. Fervel et al [12] coated Al<sub>2</sub>O<sub>3</sub>/TiO<sub>2</sub>/Cu oxide-metal mixture powders on 25CD4 steel using plasma spray method. Even though there was an increase in the amount of titanium oxide and a decrease in the hardness in the mixture, toughness increased and enhancement was recorded in the wear resistance. There was also a decrease in hardness and a reduction in porosity with Cu addition. Dejang et al [13] investigated wear and fracture toughness of Al<sub>2</sub>O<sub>3</sub>/xTiO<sub>2</sub> (x=0, 3, 13 and 20) based coatings on medium carbon steel using plasma spray method. They determined that there was a decrease in

hardness and friction coefficient with increasing TiO<sub>2</sub> amount and an increase in fracture toughness and emphasised the importance of TiO<sub>2</sub> in terms of mechanical and tribological properties of Al<sub>2</sub>O<sub>3</sub> coatings. Islak et al [14] investigated effect on the microstructure properties of TiO<sub>2</sub> rate in Al<sub>2</sub>O<sub>3</sub>-TiO<sub>2</sub> composite coating produced using plasma spray method. The results showed that the coatings had a lamellar-like structure. Besides, hardness of coating layer decreased with increasing TiO<sub>2</sub> content.

Thermal spraying technology is widely used as thermal barrier coatings and abrasion resistant coatings. Particularly, zirconia (ZrO<sub>2</sub>) coated metallic structures have superior properties as thermal barrier coatings due to their resistance to high temperatures [15]. Oxide based coatings, which are fabricated using plasma spray method in automotive industry, are successfully developed for the thermal protection of components such as piston and valve. These coatings are used to provide decreasing abrasion, wear and fraction at high temperatures [16-18].

α-Al<sub>2</sub>O<sub>3</sub> coatings produced using plasma spray method are also used for biomedical purposes. The biomaterial has to be in compliance with the place where it functions. Therefore, the modification of the surface of the biomaterial is extremely important. For example, metallic materials such as austenitic stainless steel, cobalt-chromium alloys and titanium alloys are widely used as surgical implant materials. Among them, especially AISI 316 stainless steel is cheap and easily producible and has excellent corrosion resistance. However, these austenitic stainless steels degrade by being exposed to aggressive biological effects in long-term applications. The surface properties of these materials are improved by making oxide coatings via plasma spray [19, 20].

In this study, ZrO<sub>2</sub> / Al<sub>2</sub>O<sub>3</sub>-TiO<sub>2</sub> oxide coatings were produced by using plasma spray method on AISI 304

stainless steel surface. Different amounts of  $\text{Al}_2\text{O}_3\text{-TiO}_2$  were added to  $\text{ZrO}_2$  powder. Depending on the amount of addition, microstructure and micro-hardness changes were experimentally investigated.

## 2. Experimental studies

AISI 304 stainless steel bars with a dimension of  $\text{Ø } 20 \times 100$  mm were used as the substrate.  $\text{ZrO}_2$  and  $\text{Al}_2\text{O}_3\text{-13 wt\%TiO}_2$  oxide powders with  $-90+30 \mu\text{m}$  and  $-53+15 \mu\text{m}$  grain sizes respectively were coated on the substrate using plasma spray method. Ni-20Cr (atomized in water) metallic alloy powder with  $-53+11 \mu\text{m}$  grain size was used as the bonding layer powder. Table 1 illustrates the mixture rates of the powders which are used in the coating process. Fig. 1 illustrates SEM images of the oxide powders which are used in coating, and Fig. 2 illustrates their XRD analyses. As is seen in Fig. 1, oxide powders are irregularly sharp edged, and there are differences in grain sizes. In order to form a better bonding between the metallic substrate and oxide coating, the substrate is subjected to sanding process through  $\text{Al}_2\text{O}_3$  sand with a grain size between 24-35 mesh. Nearly 20  $\mu\text{m}$ -thick Ni-20Cr bonding layer is formed between the oxide coating layer and the substrate. Finally, oxide coating with 100  $\mu\text{m}$ -thick  $\text{ZrO}_2$  and  $\text{Al}_2\text{O}_3\text{-13 wt\% TiO}_2$  powder mixture was produced on the bonding layer.

Table 1. Mixture rates of coating powders.

Specimens	Powder mixture (wt.%)	
	$\text{ZrO}_2$	$\text{Al}_2\text{O}_3 - 13 \text{ TiO}_2$
Z	100	0
ZA40	60	40
ZA60	40	60

In producing both bonding and oxide coating layer, Sulzer Metco F4-MB atmospheric plasma spray coating system with 55 kW power was used. Fig. 3 illustrates the principle scheme of plasma spray coating process. Production parameters of oxide coatings are summarised in Table 2.

For metallographic examinations, samples were taken from the section area perpendicular to coating direction. The metallographic samples obtained were treated with 80-1200 mesh sandpaper and their surfaces were cleaned.

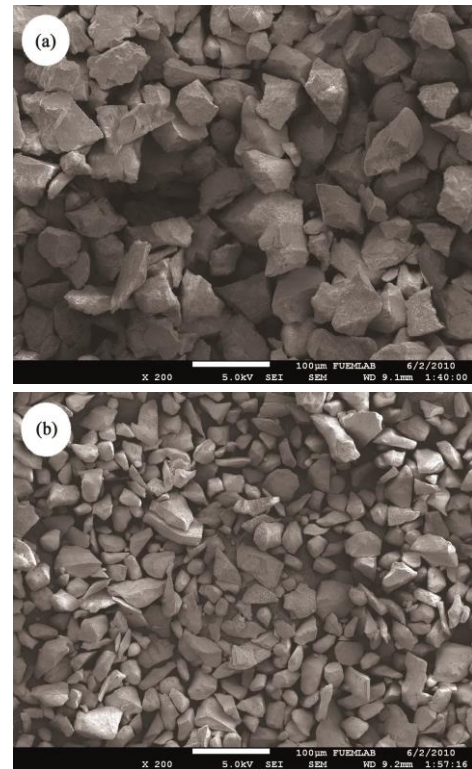


Fig. 1. SEM images of the powders used in the coating - (a)  $\text{ZrO}_2$  powder and (b)  $\text{Al}_2\text{O}_3\text{-13 TiO}_2$  powder.

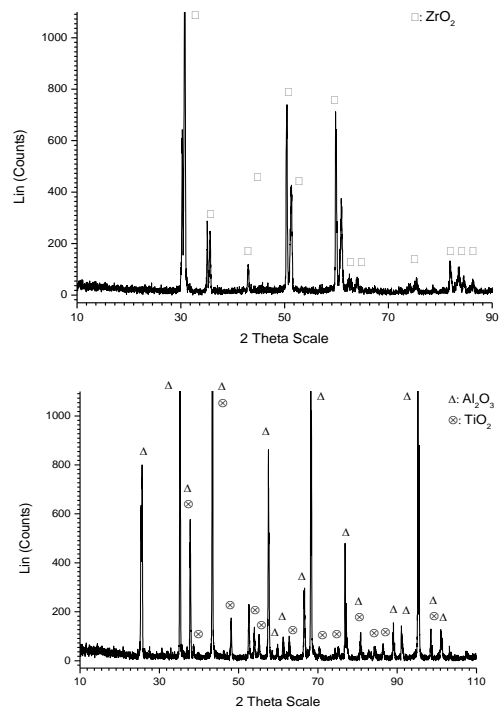


Fig. 2. XRD graphics of  $\text{ZrO}_2$  and  $\text{Al}_2\text{O}_3\text{-13 TiO}_2$  coating powder.

Then, side section surfaces were polished by means of 1 and 6  $\mu\text{m}$  diamond paste. Samples were electrolytically

etched in  $\text{HNO}_3$  and alcohol mixture solution for microstructural examinations. In each coating, scanning electron microscopy (SEM) and X-ray diffraction (XRD) analyses were used for microstructure and phase analysis. Hardness measurement was performed in 10 second dwell time under load of 200 g using Future-Tech FM 700 brand microhardness device along a line from the top surface of the coating towards the substrate.

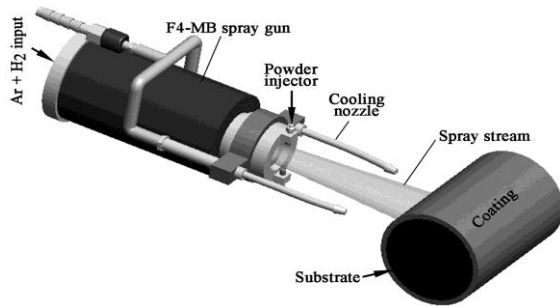


Fig. 3. Principle scheme of plasma spray coating process.

Table 2. Production parameters.

Parameters	
Plasma spray gun	Sulzer-Metco F4
Current (A)	580
Voltage (V)	60-65
Ar gas flow rate (l/min)	35
$\text{H}_2$ gas flow rate (l/min)	9-11
Spray distance (mm)	75
Powder feed rate (g/min)	45
Carrier gas flow rate (Ar) (l/min)	3.0

### 3. Results and discussion

Fig. 4 illustrates SEM images of  $\text{ZrO}_2$ ,  $\text{ZrO}_2-40(\text{Al}_2\text{O}_3-13 \text{ wt.}\% \text{ TiO}_2)$  and  $\text{ZrO}_2-60(\text{Al}_2\text{O}_3-13 \text{ wt.}\% \text{ TiO}_2)$  coatings which were fabricated using plasma spray method. The coatings generally consisted of three zones as oxide coating layer, intermediate layer and substrate. In each one of three oxide coatings, there is lamellar microstructure, which is formed in thermal spray coatings [21, 22]. The lamellar structure occurs with the strike of melted particles to the substrate, their deformation and solidification [1, 2]. According to Kuroda and Kobayashi [16], lamellae forms in parallel with the substrate and while the middle part of the lamellae is thick, the thickness reduces towards the edges. SEM images illustrate a better homogeneity in the lamellar structure with the increase of  $\text{Al}_2\text{O}_3-13\text{TiO}_2$  (Fig. 4b-c). In the  $\text{Al}_2\text{O}_3-13\% \text{ TiO}_2$  coating which was produced by Bolelli et al [23] using plasma spray, they reported that  $\text{TiO}_2$  melted and partially mixed with  $\text{Al}_2\text{O}_3$ , and the lamellar structure with different  $\text{TiO}_2$  amounts formed. They also explained that  $\text{TiO}_2$  provided a better adhesion between the splashing particles. Pore formation was observed in all of the coatings (Fig. 4). This

pore formation generally occurs in all thermal spray coatings [24-26]. Porosity originates from the insufficient filler and insufficient wetting capability of the melted particles which strike the rough coating surface [27]. The amount of pore varies based on the surface roughness of the substrate, spraying distance, substrate temperature and coating thickness [28]. In this study, the change in the pores alters based on the  $\text{Al}_2\text{O}_3-13\text{TiO}_2$  amount because the spraying parameters were selected fixed. SEM images in Fig. 4 illustrate increasing  $\text{Al}_2\text{O}_3-13\text{TiO}_2$  amount and the decrease in amount of pore. This situation is associated with the fact that thermal conductivity of  $\text{Al}_2\text{O}_3$  is higher than  $\text{ZrO}_2$  [29].

SEM images illustrate the unmelted, partially or completely melted areas in the coatings. The porosity decreased from the binding layer to the upper part of the coating. This situation happened in all of the coatings. Shanmugavelayutham and Kobayashi [30] determined that porosity decreased from the binding layer towards the upper part of the layer in zirconia-alumina based thermal barrier coatings fabricated on SUS304 steel.

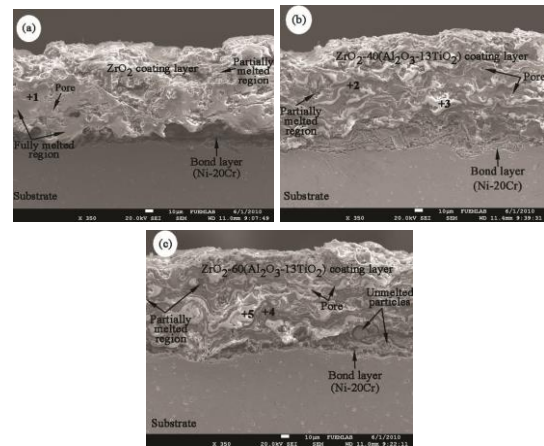


Fig. 4. SEM image of  $\text{ZrO}_2/\text{Al}_2\text{O}_3$  coatings: (a) Z coating, (b) ZA40 and (c) ZA60 coating.

Fig. 5 illustrates the EDS analysis of the points determined in the microstructure of the oxide coatings in Fig. 4. The EDS analysis of point 1 in  $\text{ZrO}_2$  coating was 55.12% Zr and 44.88 % O. The EDS analysis of point 2 in  $\text{ZrO}_2-40(\text{Al}_2\text{O}_3-13\text{TiO}_2)$  coating was 34.96 % Al, 4.56% Ti, 1.77% Zr and 58.70%; and EDS analysis of point 3 was 2.95% Al, 0.48% Ti, 52.26% Zr, and 44.31% O. The EDS analysis of point 4 in  $\text{ZrO}_2-60(\text{Al}_2\text{O}_3-13\text{TiO}_2)$  based composite coating was 35.68% Al, 8.68% Ti, 0.80% Zr and 54.85% O; and the EDS analysis of point 5 was 1.96% Al, 0.32% Ti, 57.39% Zr, and 40.33% O. The dark areas in the microstructure of these coatings (except for Z sample) are rich in  $\text{Al}_2\text{O}_3/\text{TiO}_2$ , and the light coloured areas are rich in  $\text{ZrO}_2$ . This situation is also supported by EDS analyses. Al and Ti amount in the microstructure increased in the increasing addition of  $\text{Al}_2\text{O}_3-13\text{TiO}_2$  powder.

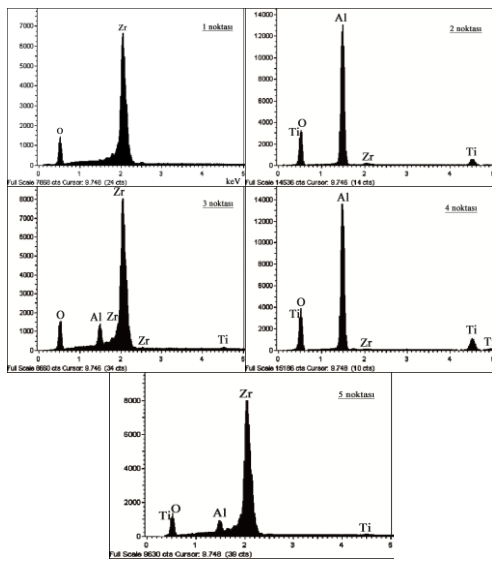


Fig. 5. EDS analysis of  $ZrO_2/Al_2O_3$  coatings.

Fig. 6 illustrates the XRD graphic of  $ZrO_2/Al_2O_3$  based composite coatings which are produced with plasma spray.  $ZrO_2$ ,  $Al_{0.52}Zr_{0.48}O_{1.74}$ ,  $ZrTiO_4$ ,  $Al_{0.18}Zr_{0.82}O_{1.91}$ ,  $Al_2O_3$ ,  $Al_2Zr_3$ ,  $Al_3Ti$  and  $Ti_2O_3$  phases formed in the coatings. The binary and ternary phases except for  $ZrO_2$  and  $Al_2O_3$  showed that the powders were homogenously mixed in order to prevent their accumulation before coating process. By this way, the contact area of the powders was increased; and thus their reaction was enabled.

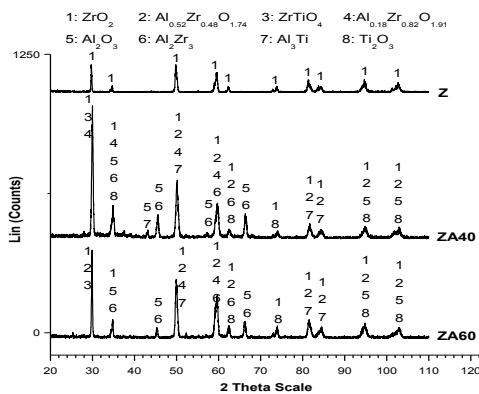


Fig. 6. XRD graphic of plasma spray coatings.

Fig. 7 illustrates the microhardness variation graphic of the plasma spray coatings based on distance. The increase in hardness was observed based on the increase in the addition of  $Al_2O_3-13TiO_2$  powder. The measured average microhardness of Z, ZA40 and ZA60 coatings were 842  $HV_{0.2}$ , 988  $HV_{0.2}$ , and 1136  $HV_{0.2}$  respectively. A 4-5 times increase was measured according to the substrate. This situation can be associated with the increase in  $Al_2O_3$ , the increase in the presence of  $Al_2O_3$  in completely melted areas and the decrease in porosity. This

is because alumina particles are harder than zirconium oxide particles [29, 30].

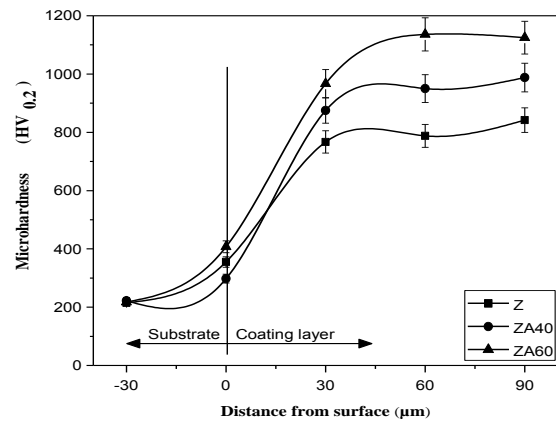


Fig. 7. Microhardness profile of oxide based coatings.

#### 4. Conclusions

Zirconia–alumina based coatings were successfully fabricated by using plasma spray method on AISI 304 stainless steel. A lamellar and layered microstructure was obtained. A small amount of non-melted particles, partially melted, completely melted areas and pores were observed in the microstructure. Decrease in pores was observed from the SEM images with the increasing addition of  $Al_2O_3-TiO_2$ . Two-and three-component phases were formed in the coatings produced using plasma spray. A 4-5 times increase was determined in the hardness values of the coatings compared to the substrate. There was an increase in the microhardness in parallel with the increase in the mixture rate of  $Al_2O_3-TiO_2$ . Average hardness was measured as 1136  $HV_{0.2}$  in coatings produced with 60 %  $Al_2O_3-TiO_2$  addition.

#### Acknowledgements

The author is grateful to Senkron Metal & Ceramics Coating Ltd Company.

#### References

- [1] R. B. Heimann, Plasma-spray coating, VCH, New York (1996).
- [2] L. Pawlowski, The science and engineering of thermal spray coatings, John Wiley & Sons, Ltd., England (2008).
- [3] D. I. Pantelis, P. Psyllaki, N. Alexopoulos, *Wear* **237**, 197 (2000).
- [4] E. P. Song, J. Ahn, S. Lee, N. J. Kim, *Surface and Coatings Technology* **202**, 3625 (2008).
- [5] A. Datye, S. Koneti, G. Gomes, K. H. Wu, H. T. Lin, *Ceramics International* **36**, 1517 (2010).
- [6] Y. Wang, S. Jiang, M. Wang, S. Wang, T. D. Xiao, P.

- R. Strutt, *Wear* **237**, 176 (2000).
- [7] G. Goller, *Ceramics International* **30**, 351 (2004).
- [8] Ş. Yilmaz, M. Ipek, G. F. Celebi, C. Bindal, *Vacuum* **77**, 315 (2005).
- [9] A. Rico, J. Rodriguez, E. Otero, P. Zeng, W. M. Rainforth, *Wear* **267**, 1191 (2009).
- [10] Y. Sun, B. Li, D. Yang, T. Wang, Y. Sasaki, K. Ishii, *Wear* **215**, 232 (1998).
- [11] M. Cadenas, R. Vijande, H. J. Montes, J. M. Sierra, *Wear* **212**, 244 (1997).
- [12] V. Fervel, B. Normand, C. Coddet, *Wear* **230**, 70 (1999).
- [13] N. Dejang, A. Watcharapasorn, S. Wirojupatump, P. Niranatlumpong, S. Jiansirisomboon, *Surface and Coatings Technology* **204**, 1651 (2010).
- [14] S. Islak, S. Buytoz, E. Ersöz, N. Orhan, J. Stokes, M. S. Hashmi, I. Somunkiran, N. Tosun, *Optoelectron. Adv. Mater. Rapid Commun.* **6**(9-10), 844 (2012).
- [15] H. Ahn, J. Y. Kim, S. S. Lim, *Wear* **203-204**, 77 (1997).
- [16] T. Kuroda, A. Kobayashi, *Vacuum* **73**, 635 (2004).
- [17] A. M. Limarga, S. Widjaja, T. H. Yip, *Surface and Coatings Technology* **197**, 93 (2005).
- [18] G. Shanmugavelayutham, S. Yano, A. Kobayashi, *Vacuum* **80**, 1336 (2006).
- [19] M. H. Fathi, M. Salehi, A. Saatchi, V. Mortazavi, S. B. Moosavi, *Dental Materials* **19**, 188 (2003).
- [20] I. Gurappa, *Surface and Coatings Technology* **161**, 70 (2002).
- [21] C. J. Li, G. J. Yang, A. Ohmori, *Wear* **260**, 1166 (2006).
- [22] C. H. Lee, H. K. Kim, H. S. Choi, H. S. Ahn, *Surface and Coatings Technology* **124**, 1 (2000).
- [23] G. Bolelli, V. Cannillo, L. Lusvarghi, T. Manfredini, *Wear* **261**, 1298 (2006).
- [24] Z. Yin, S. Tao, X. Zhou, C. Ding, *Journal of the European Ceramic Society* **28**, 1143 (2008).
- [25] X. Lin, Y. Zeng, W. S. Lee, C. Ding, *Journal of the European Ceramic Society* **24**, 627 (2004).
- [26] E. P. Song, J. Ahn, S. Lee, N. J. Kim, *Surface and Coating Technology* **202**, 3625 (2008).
- [27] C. J. Li, W. Z. Wang, *Materials Science and Engineering A* **386**, 10 (2004).
- [28] H. M. Choi, B. S. Kang, W. K. Choi, D. G. Choi, *Journal of Materials Science* **33**, 5895 (1998).
- [29] J. Zhang, A. Kobayashi, *Vacuum* **83**, 92 (2008).
- [30] G. Shanmugavelayutham, A. Kobayashi, *Materials Chemistry and Physics* **103**, 283 (2007).

---

\*Corresponding author: serkanislak@gmail.com